

# ESTIMATION OF AIR FILM THICKNESS BETWEEN MOVING WEBS AND GUIDE ROLLERS

by

H. Hashimoto  
Tokai University  
Japan

## ABSTRACT

In this paper, in order to estimate an air film thickness between moving web and guide roller (web spacing height), the air film thickness formula was derived based on the finite width compressible foil bearing theory. In the derivation of air film thickness formula, the two-dimensional Reynolds equation and foil equilibrium equation were discretized by the finite difference method and solved iteratively to obtain the pressure and air film thickness distributions for various parameters. Based on the numerical results, the simplified convenience formula for the estimation of air film thickness between web and guide roller was obtained. On the other hand, the air film thickness between web and guide roller was measured by the optical sensor, and the experimental results were compared with the calculated results. Moreover, the variation of air film thickness between layer and layer in winding processes of web was analyzed by making use of the air film thickness formula. From the theoretical and experimental results obtained, the effects of air film thickness on the web transporting systems were clarified.

## NOMENCLATURE

- $a$  = distance defined in Fig.2 (m)
- $2B$  = web wrap angle (deg)
- $h$  = air film thickness (spacing height between web and roller or air film thickness between layer and layer) (m)
- $\bar{h}$  = dimensionless air film thickness ( $=h/(R\epsilon^2)$ )
- $h_0$  = air film thickness at  $x=0$  in Fig.2 (m)
- $L$  = web width (m)
- $p$  = air film pressure (Pa)
- $\bar{p}$  = dimensionless air film pressure ( $=(p-p_a)/(T/R)$ )
- $p_a$  = ambient pressure (Pa)
- $R$  = roller radius (m)
- $t$  = web winding time (s)

$T$	=	web tension (N/m)
$u$	=	web deflection (m)
$U$	=	web traveling velocity (relative velocity) (m/s)
$x$	=	coordinate in the direction of web traveling (m)
$\bar{x}$	=	dimensionless coordinate in the direction of web traveling ( $=x/(R\varepsilon)$ )
$x_s$	=	inlet coordinate of web wrapped region in Fig.2 (m)
$x_c$	=	outlet coordinate of web wrapped region Fig.2 (m)
$z$	=	coordinate in the axial direction (m)
$\bar{z}$	=	dimensionless coordinate in the axial direction ( $=z/L$ )
$\beta$	=	dimensionless web wrap angle ( $=B\varepsilon$ )
$\varepsilon$	=	web parameter ( $=(6\mu U/T)^{1/3}$ )
$\lambda$	=	slenderness ratio of web ( $=L/(2R\varepsilon)$ )
$\mu$	=	air viscosity

## INTRODUCTION

In the manufacturing fields of plastic sheet, paper, magnetic tape, photographic film etc., the web transporting systems supported by the guide rollers are often used. Moreover, in addition to the transporting processes, the web winding processes are generally included in the systems. In such systems, it is of cardinal importance to estimate an air film thickness (lubricating air film thickness) between traveling web and guide roller or between layer and layer in the wound web for understanding the frictional conditions there and for improving the efficiency of web handling processes (1). The air film thickness formula based on the infinitely long width foil bearing theory (2,3) is generally used for the estimation of air film thickness in the web handling processes. However, in the case of small web width, the infinitely long bearing assumption will cause significant quantitative errors in the estimation of air film thickness.

In this paper, the air film thickness formula is newly developed based on the finite width compressible foil bearing theory (4,5), and the calculated results of air film thickness by the formula are compared with the experimental results. Before deriving the air film thickness formula, the two-dimensional Reynolds equation and foil equilibrium equation (4) are discretized by the finite difference method and solved iteratively to estimate the pressure and air film thickness distributions for various parameters. Based on the numerical results, the simplified convenience formula for the estimation of air film thickness between web and guide roller, which includes the web width, web tension and web traveling velocity as parameters, is obtained. On the other hand, in the experiments, the air film thickness between web and guide roller is measured by the optical sensor for various combinations of web wrap angle, web tension and web traveling velocity, and the experimental results are compared with the calculated results. Moreover, as one of applications of above derived formula, the variation of air film thickness between layer and layer in winding processes of web is analyzed by making use of the squeeze film model (6), in which the initial air film thickness is given by the air film thickness formula.

## ANALYSIS OF WEB SPACING HEIGHT

Figure 1 shows the outline of web transporting systems. A web is continuous, thin and flexible material, and it is transported through various processes such as coating, drying, printing etc., and finally it is wound. The traveling web brings the surrounding air into the gap between web and guide roller, and then the web is lifted slightly by the film pressure generated due to the air viscous effect as shown in part A. Moreover,

when the web is wound, the web brings the air into the gap between layer and layer in the wound web as shown in part B. In both cases, the common engineering problems are to estimate the air film thickness accurately for understanding the frictional conditions there. In this chapter, the analysis of web spacing height (air film thickness between web and guide roller) is described.

The foil bearing model as shown in Fig.2 is generally applied to analyze the web spacing height in Region II (web wrapped region). Assuming that the web is perfectly flexible and the web deflection in the axial direction is negligible small, the web spacing height and pressure distributions are obtained theoretically by solving the following Reynold equation and web elastic equation simultaneously.

$$\frac{\partial}{\partial x} \left( \frac{h^3 p}{12\mu} \frac{\partial p}{\partial x} \right) + \frac{\partial}{\partial z} \left( \frac{h^3 p}{12\mu} \frac{\partial p}{\partial z} \right) = \frac{U}{2} \frac{d(ph)}{dx} \quad (1)$$

$$\frac{1}{L} \int_0^L \{p(x,z) - p_a\} dz = T \left( \frac{1}{R} - \frac{\partial^2 h}{\partial x^2} \right) \quad (2)$$

As the pressure in Regions I and III is equal to the ambient pressure, it is expressed as :

$$p = p_a \quad (3)$$

Moreover, the web deflection in Regions I and III is determined from :

$$\frac{d^2 u_{I,III}}{dx^2} = 0 \quad (4)$$

The relation between the web spacing height and the web deflection in Region II is given as :

$$u_{II} = h + \sqrt{R^2 - x^2} \quad (5)$$

The boundary conditions for Reynolds equation (1) are given as :

$$\left. \begin{aligned} p(x_s, z) &= p(x_e, z) = p_a \\ p(x, 0) &= p(x, L) = p_a \end{aligned} \right\} \quad (6)$$

On the other hand, the boundary conditions for the web elastic equation (2) are given as :

$$u_I(x = -R - a) = 0, \quad u_{III}(x = R + a) = 0 \quad (7)$$

Moreover, the continuity conditions for the web between Regions I and II and Regions II and III are expressed, respectively, as follows :

$$u_I(x = x_s) = u_{II}(x = x_s) \quad , \quad \left. \frac{du_I}{dx} \right|_{x=x_s} = \left. \frac{du_{II}}{dx} \right|_{x=x_s} \quad (8 \cdot a)$$

$$u_{II}(x = x_e) = u_{III}(x = x_e) \quad , \quad \left. \frac{du_{II}}{dx} \right|_{x=x_e} = \left. \frac{du_{III}}{dx} \right|_{x=x_e} \quad (8 \cdot b)$$

In the numerical analysis of governing equations mentioned above, the following nondimensional quantities are introduced to normalize the equations.

$$\left. \begin{aligned} \varepsilon &= \left( \frac{6\mu U}{T} \right)^{\frac{1}{3}} \quad , \quad \bar{x} = \frac{x}{R\varepsilon} \quad , \quad \bar{h} = \frac{h}{R\varepsilon^2} \quad , \quad \lambda = \frac{L}{2R\varepsilon} \quad , \\ \bar{p} &= \frac{p - p_a}{T/R} \quad , \quad \bar{z} = \frac{z}{L} \quad , \quad \beta = \frac{B}{\varepsilon} \quad , \quad \bar{a} = \frac{a}{R\varepsilon} \end{aligned} \right\} \quad (9)$$

Discretizing the normalized governing equations by the finite difference method and solving them with boundary conditions and continuity conditions, the web spacing height and pressure distributions are obtained.

Figure 3 shows the numerical results of web spacing height and pressure distributions for  $\lambda=4$  and 9 and  $\beta=9$ . As can be seen in the figure, the web spacing height and the air film pressure in the central region (Region II) take nearly constant values, and the local contraction of web and pressure spike generate near the outlet of Region II.

Figure 4 shows the variation of web spacing height with wrap angle for various values of slenderness ratio  $\lambda$ , in which the thick lines show the results considering the air film compressibility and the thin lines the results neglecting the compressibility, respectively. The web spacing height increases with an increase of wrap angle  $\beta$  and it becomes constant for  $\beta > 6.0$ . In the actual application of web transporting systems, the value of  $\beta$  is generally larger than 6.0. Therefore, it is considered that the web spacing height is independent of web wrap angle  $\beta$  for  $\beta > 6.0$ .

Figure 5 shows the variation of web spacing height with slenderness ratio for  $\beta > 6.0$ , in which the results by four kinds of theory are compared. The results by the finite width foil bearing theories increase with an increase of slenderness ratio and finally reach the results by the infinite width theories. The results by the incompressible or the infinite width foil bearing theories overestimate the web spacing height.

In Fig.5, applying the curve fitting technique to the numerical results based on the finite width compressible foil bearing theory, the following formula for the web spacing height is obtained.

$$h_0 = R \left( \frac{6\mu U}{T} \right)^{\frac{2}{3}} \left( 0.589 - \frac{1.614}{\lambda} + \frac{1.764}{\lambda^2} \right) \quad ; \quad \lambda = \frac{L}{2R} \left( \frac{6\mu U}{T} \right)^{-\frac{1}{3}} \quad (10)$$

## EXPERIMENTS FOR WEB SPACING HEIGHT

To confirm the applicability of Eq.(10) for the estimation of web spacing height, the calculated results by Eq.(10) are compared with the experimental results. Figure 6 shows the outline of experimental apparatus for measuring the web spacing height. The audio-tape in width of 6(mm) is used as web, which is send from the unwinding reel ①

and wound finally in the winding reel ②. The web traveling velocity is controlled by DC motor to maintain the constant traveling velocity. The web tension is generated by the lever combining the spring. The radius of guide roller (shaft) is 0.02(m) and the wrap angle of web can be set by selecting the position of guides as  $2B=66$  deg, 110 deg and 140 deg. The surface roughness height of guide roller is finished within  $1.0(\mu\text{m})$ . The web spacing height from the surface of guide roller is measured by the contactless optical sensor set just under the guide roller.

Figure 7 shows the relation between the web spacing height and the web traveling velocity for  $T=33.3(\text{N/m})$  and  $2B=66$  deg, in which the experimental results are compared with the calculated results. In both results, the web spacing height increases with an increase of web traveling velocity and the experimental results agree well with the calculated results by Eq.(10), which is derived based on the finite width compressible foil bearing theory. The results by the infinite width foil bearing theories and the results by the incompressible foil bearing theories overestimate the web spacing height.

Figure 8 shows the relation between the web spacing height and the wrap angle for  $T=33.3(\text{N/m})$  and  $U=10(\text{m/s})$ . As can be seen in the figure, the sensitivity of wrap angle on the web spacing height is small. Fairly good agreements are seen between the experimental results and the calculated results by Eq.(10).

The variation of web spacing height with web tension is shown in Fig.9 for the case of  $2B=110$  deg and  $U=10(\text{m/s})$ . The web spacing height decreases with an increase of web tension. The calculated results by Eq.(10) slightly overestimate the web spacing height.

Figure 10 shows the variation of web spacing height in the axial direction of guide roller for  $2B=110$  deg,  $U=10(\text{m/s})$  and  $T=33.3(\text{N/m})$ . The experimental results show that the web spacing height decreases slightly at the both edges of web but the amount of a decrease is insignificant. Fairly good agreements are seen between the experimental results and the calculated results by Eq.(10).

It follows from these four figures that Eq.(10), which is derived based on the finite width compressible foil bearing theory, is applicable to estimate the web spacing height under various operation conditions within a reasonable accuracy.

## APPLICATION TO WEB WINDING PROBLEMS

To estimate the air film thickness between layer and layer in the wound web is an important tribological problems in the web handling processes. As a means of analysis for the web winding problems, the squeeze film model as shown in Fig.11 may be used reasonably(6). In the winding processes, it is considered that the squeezing velocity  $\partial h / \partial t$  is relatively small and the flow in the circumferential direction is much smaller than the flow in the axial direction. Under such conditions, neglecting the compressibility of air film and the flow in the circumferential direction, the Reynolds equation for the squeeze film is expressed as follows :

$$\frac{\partial}{\partial z} \left( h^3 \frac{\partial p}{\partial z} \right) = 12\mu \frac{\partial h}{\partial t} \quad (11)$$

The boundary conditions for the air film pressure and the initial condition for the air film thickness are given, respectively, as follows:

$$p(x = -L/2) = p(x = L/2) = p_a \quad (12)$$

$$h(t = 0) = h_0 \text{ (given by Eq.(10))} \quad (13)$$

Solving Eq.(11) analytically with the conditions in Eqs.(12) and (13), the relation between the web spacing height and the web winding time is obtained as follows :

$$h(t) = \left( \frac{1}{h_0^2} + \frac{2T}{\mu RL^3} t \right)^{-\frac{1}{2}} \quad (14)$$

Figure 12 shows an example of calculated air film thickness in the wound web for  $R=0.02(\text{m})$ ,  $U=12(\text{m/s})$  and  $T=30(\text{N/m})$ . The air film thickness decreases quickly with a progress of winding time and reaches finally constant value (residual air film thickness). As can be seen in the figure, the residual air film thickness depends strongly on the web width, and the air film thickness decreases with a decrease of web width.

## CONCLUSIONS

From the theoretical and experimental works described above, the following conclusions were obtained about the air film thickness between web and guide roller or between layer and layer in the wound web.

1. The air film thickness between web and guide roller (web spacing height) is estimated reasonably by the simple formula based on the finite width compressible foil bearing theory.
2. Fairly good agreements are seen between the measured web spacing height and the calculated ones by the formula developed.
3. The air film thickness between the layer and layer in the wound web may be estimated reasonably by applying the squeeze film model, in which the initial film thickness is given by the web spacing height formula developed.

## REFERENCES

1. King, S.L., Funk, B.A., and Chambers, F.W., "Air Films Between a Moving Tensioned Web and a Stationary Support Cylinder," Proc. of Int. Conf. of Web Handling, 1994.
2. Eshel, A., and Elrod, H.G., "The Theory of Infinitely Wide Perfectly Flexible Self-Acting Foil Bearings," Trans. ASME, Jour. Basic Engineering, Vol. 87, 1965, pp. 831-836.
3. Eshel, A., "Compressibility Effects on the Infinitely Wide, Perfectly Flexible Foil Bearing," Trans. ASME, Jour. Lubr. Technol., 1968, pp. 221-225.
4. Hashimoto, H., "Theoretical Analysis of Experimentally Pressurized Porous Foil Bearings —Part I: In the Case of Smooth Surface Porous Shaft," Trans. ASME Jour. of Tribology, Vol. 117, No. 1, 1995, pp. 103-111.
5. Hashimoto, H., "Effects of Foil Bending Rigidity on Spacing Height Characteristics of Hydrostatic Porous Foil Bearings for Web Handling Processes," ASME Paper, 96-Trib32, 1996, pp. 1-6.
6. Smith, D.P., "Influence of Speed on Tape Winding in Data Cartridge Tape Systems," Proc. of Japan Int. Tribology Conf., 1990, pp. 1899-1903.



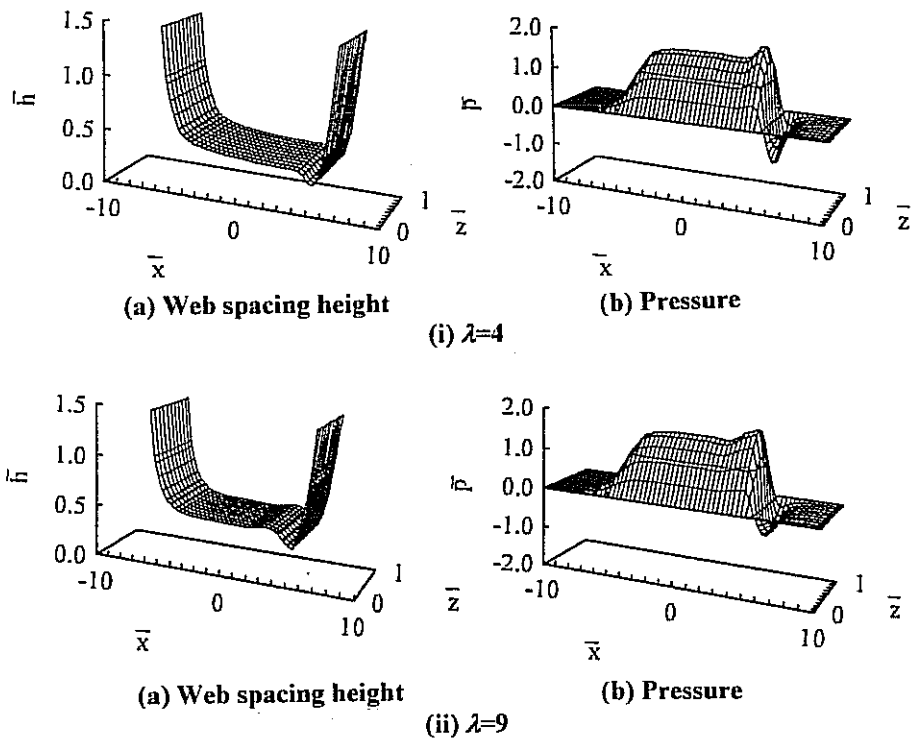


Fig.3 Web spacing height and pressure distributions for  $\beta=9$

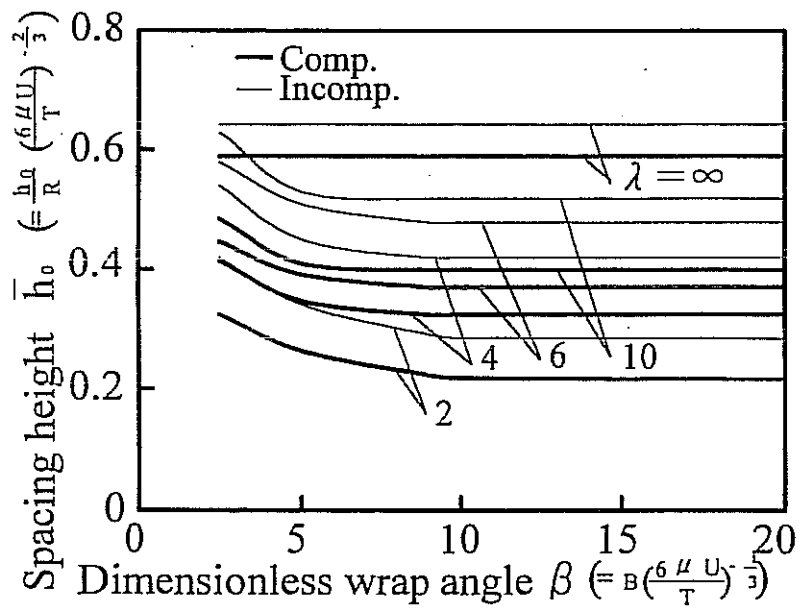


Fig.4 Variation of web spacing height with wrap angle for various values of  $\lambda$



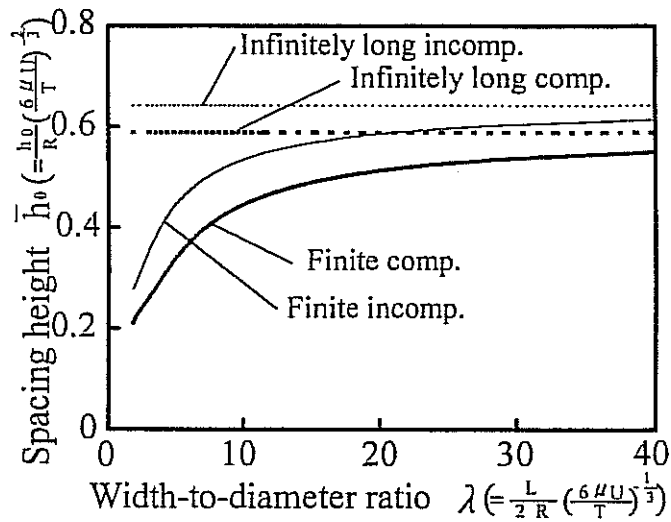


Fig.5 Variation of web spacing height with slenderness ratio for  $\beta > 6.0$

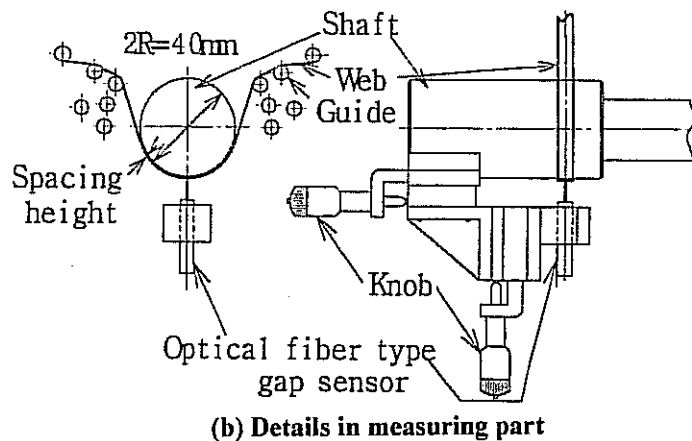
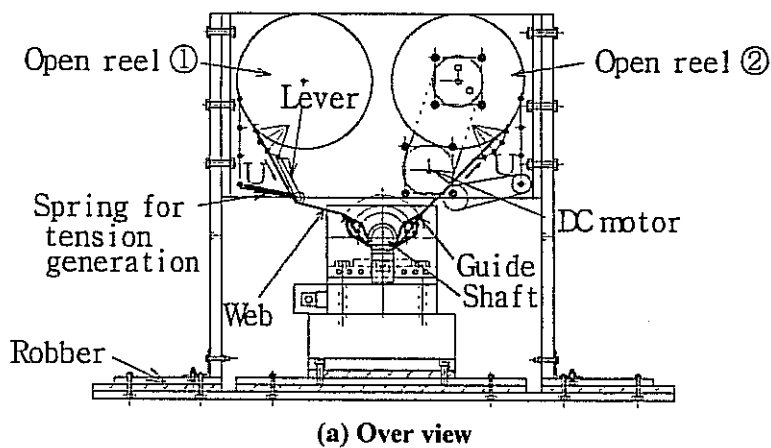


Fig.6 Experimental apparatus for measuring web spacing height

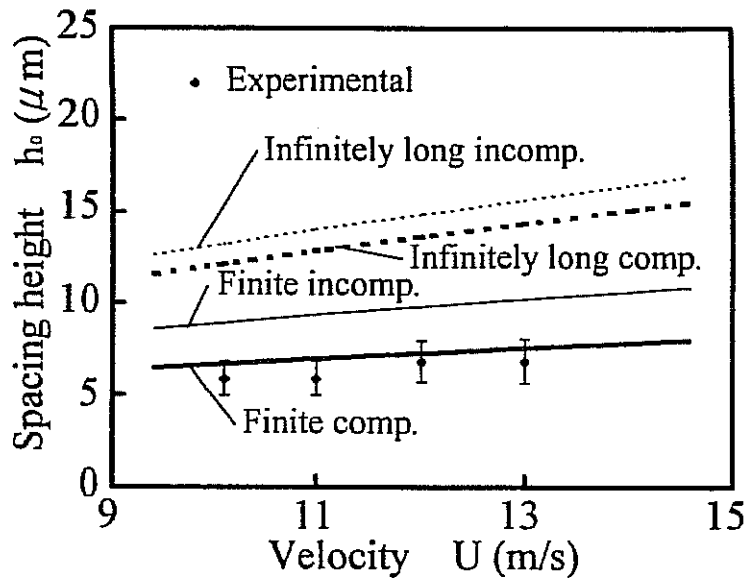


Fig.7 Variation of web spacing height with web traveling velocity for  $T=33.3(\text{N/m})$  and  $2B=66$  deg.

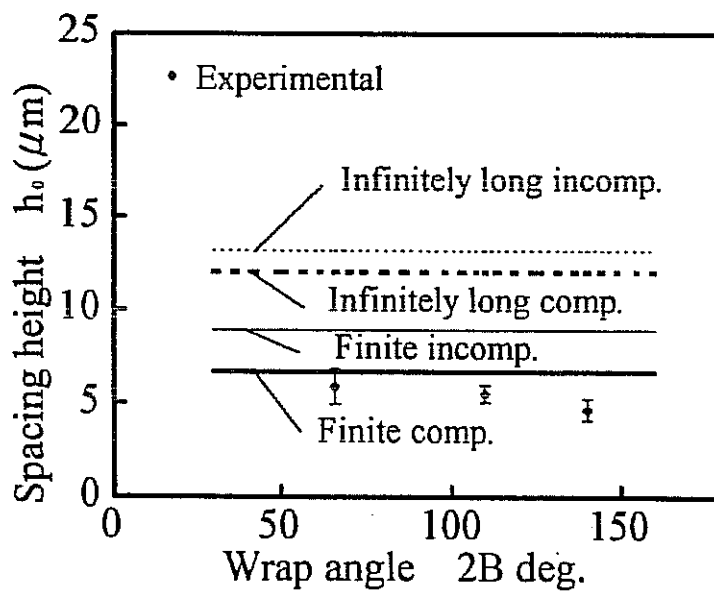


Fig.8 Variation of web spacing height with wrap angle for  $T=33.3(\text{N/m})$  and  $U=10(\text{m/s})$

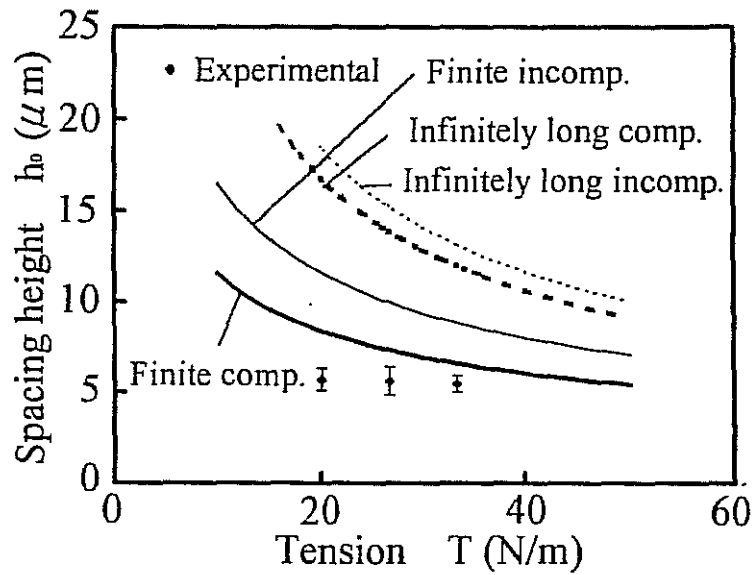


Fig.9 Variation of web spacing height with web tension for  $2B=110$  deg. and  $U=10(\text{m/s})$

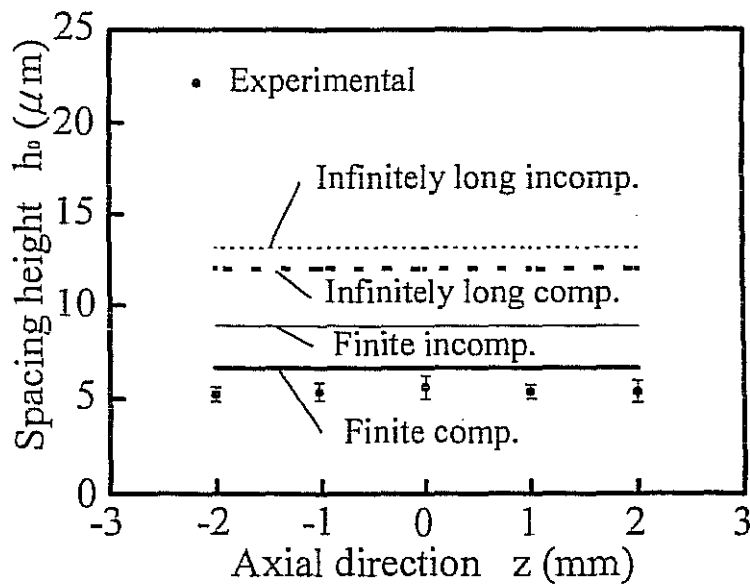


Fig.10 Variation of web spacing height in the axial direction of guide roller for  $2B=110$  deg.,  $U=10(\text{m/s})$  and  $T=33.3(\text{N/m})$

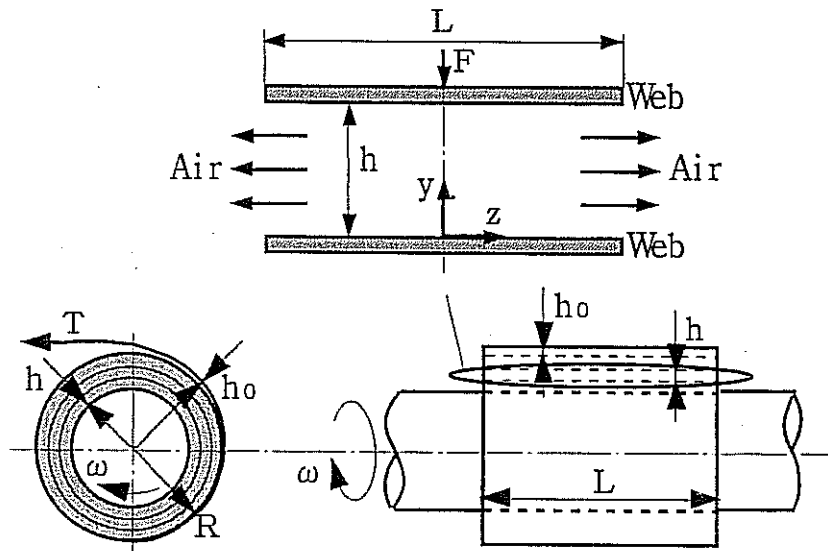


Fig.11 Squeeze foil model for analyzing web winding problem

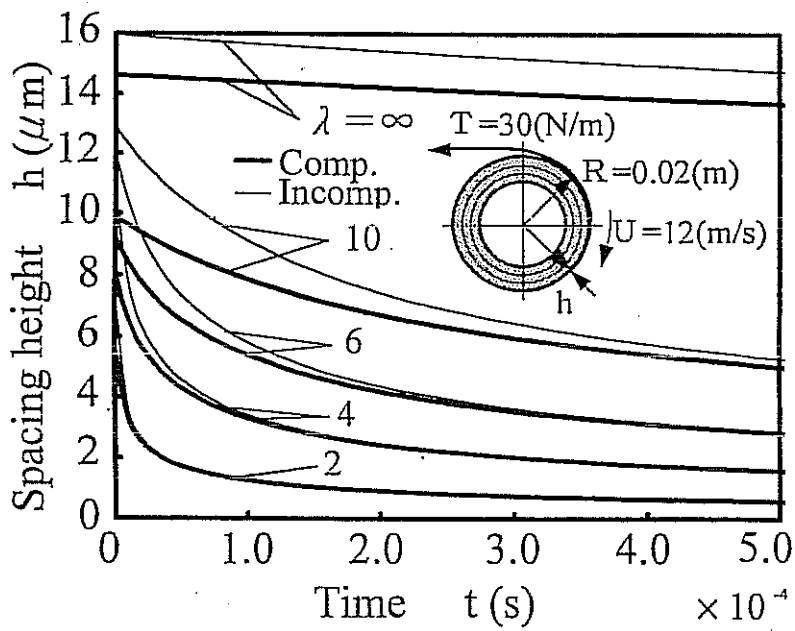


Fig.12 Variation of air film thickness with winding time for  $R=0.02(m)$ ,  $U=12(m/s)$  and  $T=30(N/m)$